

Highlights (for review)

Highlights:

1. It was the first time 7 operating modes were achieved on the same engine.
2. 7 operating modes covers conventional spark ignition and advanced controlled autoignition in two-stroke and 4-stroke cycles.
3. The thermodynamic cycle, combustion process and efficiencies are analysed and presented.

Investigation of Combustion, Performance and Emission Characteristics of 2-stroke and 4-stroke spark ignition and CAI/HCCI Operations in a DI gasoline

Y. Zhang and H. Zhao

Centre for Advanced Powertrain and Fuels (CAPF)

School of Engineering and Design

Brunel University London, UK

ABSTRACT

In order to develop more efficient and cleaner gasoline engines, a number of new engine operating strategies have been proposed and researched on different engines, including the spark ignition (SI) and controlled autoignition (CAI) or HCCI in both 2-stroke and 4-stroke cycles in a poppet valve engine. In this work, a single cylinder direct injection gasoline engine equipped with an electro-hydraulic valve-train system has been commissioned and used to achieve seven different operating modes, including: 4-stroke throttle-controlled SI, 4-stroke intake valve throttled SI, 4-stroke positive valve overlap SI, 4-stroke negative valve overlap CAI, 4-stroke exhaust rebreathing CAI, 2-stroke CAI and 2-stroke SI. Their performance and emission characteristics were analysed and compared at a typical engine calibration operating condition of 1500rpm and 3.6bar IMEP in 4-stroke or 1.8bar IMEP in 2-stroke. Results show that 4-stroke positive valve overlap SI, 4-stroke NVO CAI and exhaust rebreathing CAI modes have better fuel economy and lower NO_x emissions than the conventional throttled 4-stroke SI operation. The 2-stroke CAI operation was found to produce higher combustion efficiency and lower ISFC but lower brake efficiency than the 4-stroke operations at the same power output due to the supercharger's efficiency. But, at the same IMEP as the 4-stroke operation, the 2-stroke CAI operation results in 29% reduction in BSFC, indicating its potential synergy with highly downsized direct injection gasoline engines for much better fuel economy and performance.

INTRODUCTION

Gasoline engines are the dominant power plant for passenger cars due to their low emission and superior performance. In order to meet the new legislation on CO₂ emission and fuel economy being introduced in Europe, US, Japan, China and many other countries, it is imperative to improve the efficiency and reduce fuel consumption of gasoline engine powered vehicles. It is known that the poorer fuel economy of the gasoline engine is caused by operating at a lower compression ratio in order to avoid knocking combustion at full load and with the stoichiometric air/fuel ratio for stable combustion and efficient aftertreatment. However, as the engine in a passenger car is operated at part-load in most driving conditions, the pumping loss of the gasoline engine at part-load has the most significant effect on the overall fuel economy. In addition to engine downsizing, Variable valve actuation (VVA) technology is considered as one of the key engine technologies by the automotive industry due to its potential for improved performance, better fuel economy and lower emissions through both optimised gas exchange and advanced combustion technologies. The simplest and most widely used VVA technology is the Variable Valve Timing (VVT) system. Combined with optimized cam profiles, VVT has been used to achieve improved gasoline engine performance and lower exhaust emissions. In addition, the cam profile switching (CPS) device has been developed and applied to some high performance gasoline engines, which allows a switch between two discretely different cam profiles optimized for better fuel economy at low load and high load performance respectively. By the end of 1990's, mechanical fully variable valvetrains were developed, e.g. BMW Valvetronics system [1] and several other manufacturers have developed their own continuous variable mechanical valve lift devices over the last few years [2-5]. More recently, Fiat introduced the most flexible production VVA system, the electro-hydraulic actuated multi-air VVA, in their production engines. The multi-air VVA enables the intake valve lift and timing to be varied continuously during the intake process. It is also capable of opening the intake valve during the exhaust stroke. Those variable valve lift/timing devices enable the unthrottled engine load control to be realised by using intake valve throttling. In the meantime, camless valvetrains, such as electro-magnetic and electro-hydraulic valve system, have been developed mostly for single cylinder engine studies in the laboratory environment [6-8].

The development and application of VVA technology has enabled new engine cycle and combustion processes to be investigated and evaluated for improved fuel efficiency and lower exhaust emissions. One of the most significant combustion processes is the Controlled Auto-ignition (CAI) or HCCI combustion [9]. Many approaches have been attempted to achieve CAI operation on the four-stroke spark ignition engines, such as intake air heating, high compression ratio, dual fuel, recycling the exhaust gas, and so on [10]. Amongst these approaches, internally

recycling the exhaust gas has been proved most effective in achieving CAI combustion in the 4-stroke cycle. Lotus Engineering demonstrated the operational range of CAI through residual gas trapping in a single cylinder gasoline engine and mode switches between SI and CAI combustion using their fully flexible AVT camless system [11]. AVL demonstrated that CAI/HCCI combustion could also be realised in a direct injection gasoline engine by exhaust gas rebreathing using a set of electro-hydraulic valves to reopen the exhaust valve during the intake process [12]. FEV presented and discussed the fuel consumption and emissions of different exhaust gas recirculation methods achieved by an electromechanical valvetrain [13]. In order to extend the load range of CAI combustion for automotive applications, 2-stroke CAI combustion in a 4-valve direct injection gasoline engine was proposed and researched [14]. In order to overcome the high HC and CO emissions and durability issues associated with the conventional crankcase scavenged 2-stroke engines, the 2-stroke poppet valve engine has been developed using the same engine architecture as the current 4-stroke engine, as part of a consortium in developing 2/4 stroke switchable engine technologies through engine downsizing [15]. In addition, direct fuel injection is applied to avoid short-circuiting fuel during the scavenging process. Controlled Auto Ignition is initiated by residual gases trapped in the cylinder through incomplete scavenging, which is inherent to the 2-stroke operation.

In this paper, the 2/4 stroke switchable single cylinder direct injection gasoline engine and its instrumentation will be presented first. This is followed by a description of the 7 different engine operating modes that were implemented and tested at a typical operation condition of 1500rpm at 3.6bar IMEP in 4-stroke or 1.8bar IMEP in 2-stroke cycle. The in-cylinder pressure measurement and exhaust emission analysis are presented and discussed for the 7 operating modes.

EXPERIMENTAL SETUP

The engine used in this work is a single cylinder gasoline engine as shown in Figure 1 and its specifications are given in Table 1. Four electro-hydraulic actuators are installed on the cylinder head to enable independent control of the timings and lifts of the 4 valves. They are supplied with hydraulic fluid at 100bar by a high pressure hydraulic pump system. The fuel is injected directly into the cylinder by a Denso slit-type injector mounted under intake ports at an injection pressure of 100bar. The cylinder head features vertical intake runner and ports so that a reversed tumble flow can be set up in the cylinder. The reversed tumble forces the intake air to enter the combustion chamber on the opposite site to exhaust valves and reach exhaust valves at the end of its rotation in order to avoid the air short-circuiting during the intake and exhaust valve overlap period during the 2-stroke cycle operation. An instantaneous fuel flow meter is installed between the high pressure fuel pump and injector for the measurement of fuel flow rate. An external supercharger system is connected to the engine's intake system to supply the compressed air at a pre-set boost pressure and temperature through closed loop control of heaters and heat exchangers. A laminar air flow meter is installed in the engine's intake system to measure the intake mass flow rate. The intake and exhaust pressures were measured by two piezo resistive pressure transducers. Exhaust emissions were measured by a Horiba 7170DEGR system which sampled the exhaust gases from the exhaust manifold. The instantaneous in-cylinder pressure was measured by a piezo-electric pressure transducer and pegged onto the intake pressure at Intake Valve Closing (IVC), and then the heat release and combustion characteristics could be calculated and displayed on-line using an in-house Labview data acquisition and combustion analysis programme. The engine is mounted on a dynamic engine testbed with fully automated coolant and oil conditioning circuits and driven by an AC motor so that both motored and fired operation could be performed. The engine brake torque was measured by a torque transducer installed on the dynamometer. Uncertainties of all measurement variables are listed in Appendix.

OVERVIEW OF THE ENGINE OPERATING MODES

In this work, seven engine operation modes were achieved through different combinations of valve timings and durations. Figure 2 shows the valve timings and injection timings used in different operation modes. In addition, during the 4-stroke mode operations, the supercharger was turned off and the intake air was drawn from ambient. For the 2-stroke mode operations, the compressed air supply from the supercharger was connected to the intake system to provide the boost air.

MODE 1: 4-STROKE THROTTLE-CONTROLLED SI MODE

This is the conventional spark ignition mode used in the production gasoline engine. Engine load is controlled by the throttle opening, and its combustion process is initialized by the spark discharge followed by flame propagation. The engine was operated in this mode to obtain the baseline data. At part load, the partially closed throttle results in significant increase in the pumping loss, the main cause for the poor fuel economy of current SI gasoline engines. In this engine operation mode, the fuel was injected earlier in the intake stroke to obtain a homogeneous mixture. To prevent wetting the piston crown, the start of injection timing used in this paper was set to 300 deg. CA before combustion Top Dead Centre (TDC).

MODE 2: 4-STROKE INTAKE VALVE THROTTLED SI MODE

In order to reduce the pumping loss caused by the partially closed intake throttle at part load, intake valve opening duration can be used to regulate the amount of air into the cylinder with Wide Open Throttle (WOT). In this work, the

intake valve opening (IVO) was fixed at normal timing and the intake valve closing (IVC) was varied to throttle the intake air flow.

MODE 3: 4-STROKE POSITIVE VALVE OVERLAP SI MODE

In this case, IVO takes place before TDC and EVC after TDC to create a positive overlap between the intake and exhaust valve opening period. As the intake valve opens in the exhaust stroke, a portion of exhaust gas enters the intake port and will be sucked back into the cylinder in the intake stroke. The exhaust valve closes after TDC so that some exhaust gas will be sucked back into cylinder. In this work, the intake and exhaust valve lifts were reduced to 3mm to avoid the contact of the piston and valves around the gas exchange TDC. The intake throttle was used as the principal means to control the engine load but it was adjusted to a wider opening position than that of 4-stroke throttle-controlled SI operation in order to trap the correct amount of air in the cylinder with the recycled exhaust gas present.

MODE 4: 4-STROKE NEGATIVE VALVE OVERLAP CAI MODE

Another way to obtain internal EGR is to trap a portion of the burnt gas in the cylinder by earlier closing of the exhaust valve. To minimize backflow the intake valve opening is retarded. A negative valve overlap period is formed and the residuals are recompressed around the gas exchange TDC. In this case, intake air flow rate is dependent on the amount of the trapped residuals, which can be controlled by varying exhaust valve closing. Therefore, the throttle can be kept wide open and hence the pumping losses reduced. As the exhaust valve closes earlier, the fuel injection timing can be advanced into the exhaust stroke for better evaporation and atomization. In this work, the start of fuel injection timing was fixed at 440deg CA before combustion TDC.

MODE 5: 4-STROKE EXHAUST REBREATHING CAI MODE

Another way to obtain the internal EGR is to secondarily open the exhaust valve during the intake stroke, so a portion of the exhaust gas can be sucked back into the cylinder from the exhaust manifold. This increases the challenge to the valve system as the exhaust valve needs to open twice within one engine cycle. To achieve this valve event, in this work, the two exhaust valves were actuated individually. One exhaust valve opened as normal and the other one in the intake stroke. The air flow rate in this mode was also controlled by the intake valve duration with WOT.

MODE 6: 2-STROKE CAI MODE

The engine was switched to the 2-stroke cycle operation by opening both intake and exhaust valves around BDC in each crankshaft revolution. The boosted intake air forces the exhaust gas out during the valve overlap period through the so-called scavenging process. By altering the valve overlap period, the scavenging efficiency and hence the amount of residual gases trapped in the cylinder can be varied. In order to achieve CAI combustion in this work, exhaust valves were closed earlier so that the scavenging process was less complete and more residual gases were trapped in the cylinder. In this operation mode the engine load was determined by the boost pressure. Fuel was injected after the exhaust valve closing and before the intake valve closing for better mixing through longer mixture preparation period and the interaction between the intake air and fuel injection. The start of injection timing was set to 140deg CA BTDC.

MODE 7: 2-STROKE SI MODE

As a basis for comparison, the 2-stroke SI mode was also studied in this work. It was realised by extended exhaust period to maximise the scavenging efficiency. Engine load was also determined by the boost pressure. As less burnt gas was retained in the cylinder, the boost pressure requirement was reduced at the same engine load compared to the 2-stroke CAI mode.

RESULTS AND DISCUSSION

In order to compare the results in different operating modes, the engine was operated at a typical part-load operation condition of 3.6bar IMEP at 1500rpm in 4-stroke cycle. In the case of the 2-stroke cycle, the equivalent condition will be 1.8 bar IMEP at 1500rpm if the 4-stroke engine is replaced with a 2-stroke cycle engine of the same displacement volume. In this case, all 7 modes will be characterized with the same power output and their in-cylinder pressure traces are grouped together in Fig.3a. Alternatively, since the 2-stroke cycle operation can produce twice as much the power of the 4-stroke cycle engine of the same displacement volume, it will be advantageous to replace the 4-stroke engine with a 2-stroke engine of the half of the displacement volume following the engine downsizing route. In this case, the equivalent load point will be 3.6 bar IMEP at 1500rpm. Fig.3b shows the corresponding in-cylinder pressure traces of the 7 operation modes at 3.6bar IMEP.

In all 4-stroke engine experiments, the air fuel ratio was measured by a lambda sensor in the exhaust port and maintained at stoichiometric according to the lambda sensor output. In the case of spark ignition combustion operations, MBT was determined for each condition and their values are given in Table 2. In the case of the 2-stroke cycle operations, fuel rich combustion was detected due to the presence of air short-circuiting when the closed-loop

stoichiometric control based on the exhaust lambda was applied [16]. Thus, intake pressure was increased to achieve the lowest fuel consumption in the 2-stroke cycle operations, which were found to operate with near stoichiometric in-cylinder air and fuel mixtures [17].

First, it is noted that there are significant differences in the in-cylinder gas pressure in the compression stroke as different amount of charge is present in the cylinder. It can be seen from Fig. 3a that the pressure value of the 3 CAI operations (4-stroke Exhaust Rebreath, 4-stroke Negative Valve Overlap and 2-stroke CAI) are higher than those of SI operations due to the presence of the residuals in the cylinder. Compared with the 4-stroke negative valve overlap CAI combustion, the 4-stroke rebreathing CAI operation has longer valve durations. Therefore, more charge is inducted into the cylinder because of the inertia of the intake air and burnt gas flow. In the case of 2-stroke CAI operation, the charge in the cylinder is less than that of 4-stroke CAI due to the shorter effect compression stroke caused by the scavenging. In SI operations, 2-stroke SI and 4-stroke Positive Valve Overlap were unthrottled and the residuals were present. As a result, their pressure values were higher than the 4-stroke throttled SI and Intake Valve Throttled SI. In the case of operations at the same IMEP value, Fig.3b, the pressure during 2-stroke CAI compression stroke became higher as some of the residual gases were replaced by the fresh air, of which the specific heat ratio is higher than that of burnt gases. However, in 2-stroke SI operation, the compression pressure remained the same as that of 1.8bar IMEP, indicating the amount of gas charge in the cylinder didn't change but the composition ratio did and the injection quantity was doubled compared to 1.8bar IMEP case.

The heat release rates in each operating mode also reflect the difference between combustion processes taking place in the cylinder. As shown in Fig.4a and Fig.4b, CAI combustion is characterized by a faster and higher heat release rate than the SI combustion in both 2-stroke and 4-stroke operations as multipoint autoignition combustion takes place in the cylinder. In addition, 2-stroke CAI combustion occurs earlier than the 4-stroke CAI combustion because of the higher temperature of the residual gases due to the shorter period of heat transfer in the 2-stroke cycle. In the 4-stroke rebreathing CAI operation, the burnt gas in the exhaust port was sucked back in the cylinder. The residual gas temperature was lower than that of 4-stroke NVO CAI. As a result, the start of combustion and heat release process were later than that of 4-stroke NVO CAI. Furthermore, there is little difference between the 4-stroke throttled SI and 4-stroke intake valve throttled SI operations.

GAS EXCHANGE EFFICIENCY

The pressure-volume diagrams are shown in Fig. 5 for the seven operation modes at the same power output. As mentioned previously, in the conventional throttle controlled SI mode, higher pumping work occurs as a vacuum is created in the intake system at part-load by the partially closed throttle. To quantify the pumping work in the seven operating modes, Pumping Mean Effective Pressure (PMEP) was calculated from the in-cylinder pressure data during the gas exchange process. As shown in Fig. 6, when the throttle is replaced by the intake valve to control the engine load, PMEP is reduced by 0.2bar, which contributes 4% gain in gas exchange efficiency as shown in Figure 7. The PMEP is further reduced in the 4-stroke positive valve overlap SI mode. In the 4-stroke negative valve overlap mode, PMEP slightly increases due to the heat loss during the recompression process. The PMEP of the 4-stroke exhaust rebreathing mode is the lowest because of almost zero intake and exhaust pressure difference. Therefore, the gas exchange efficiency is nearly 100% in this mode. In 2-stroke operation modes, the pumping loss during the gas exchange process is zero, but the energy consumed by the supercharger is calculated and included in the Friction Mean Effective Pressure (FMEP) shown in the section of Mechanical efficiency and Brake Specific Fuel Consumption.

COMBUSTION EFFICIENCY

The combustion efficiency has been calculated from the fuelling rate and emissions data (the equations are shown in Appendix) and shown in Fig.8 in order to understand the effect of gas exchange and mixture in different operation modes on the completeness of combustion. It can be seen that the combustion efficiency of 4-stroke intake valve throttled SI is lower than that of the other four 4-stroke modes due to the lower in-cylinder temperature which reduces combustion speed and increase combustion duration, which seems to be supported by the higher CO emission measured in this operating mode.

In the 4-stroke exhaust rebreathing mode, the exhaust gas is sucked into the cylinder during the intake stroke. This upsets the air motion produced from the vertical intake port and reduces the intensity of mixing process in the cylinder, which results in inhomogeneous mixtures and hence higher CO emission seen in Fig.9 as well as the second lowest combustion efficiency amongst 4-stroke modes. Combustion efficiency of the 4-stroke negative valve overlap is the highest because of the longer mixing time after the early fuel injection in the exhaust stroke, as well as the higher charge temperature.

The 2-stroke spark ignition combustion at both part-load conditions has the lowest combustion efficiency amongst all operations. This is caused by less mixing time and inhomogeneous mixture due to the retarded injection timing at 140 deg. CA BTDC as well as incomplete flame propagation combustion in the presence of a certain amount of residual gases, which is evidenced by the highest CO and uHC emissions in Figure 9. However, the CAI combustion in the 2-stroke cycle leads to significant improvement in the combustion efficiency over the SI combustion because of the

better atomization and evaporation of the fuel injected in the hot atmosphere in the cylinder and its fast heat release rate, which results in much lower CO and uHC emissions as well.

THERMODYNAMIC EFFICIENCY

Figure 10 shows the gross indicated thermodynamic efficiency of the seven modes, which is calculated from the ratio of the gross work in the compression and expansion stroke to the heat released from the combustion process (The equation is shown in Appendix). A lot of factors can affect the thermodynamic efficiency of the internal combustion engine, such as the effective compression ratio, expansion ratio, combustion phase and duration, specific heat ratio and heat transfer to the wall. The results show very similar thermodynamic efficiencies between 4-stroke throttle controlled SI and intake valve throttled SI mode, since their combustion phase and duration are almost identical as shown in Figure 4. In 4-stroke positive valve overlap SI mode, the presence of burnt gas slows down the flame propagation speed and hence the lower thermodynamic efficiency. Figure 4 also shows that the combustion duration of 4-stroke negative valve overlap CAI and exhaust rebreathing CAI modes are shorter than that of 4-stroke SI mode, which tends to increase the thermodynamic efficiency of such operating modes as the heat addition process becomes akin to the constant volume process. In addition, low combustion temperature in the CAI modes also contributes to the high thermodynamic efficiencies seen for such operations.

In 2-stroke cycle modes, the low thermodynamic efficiency is mostly caused by the low effective expansion ratio due to the early opening of the exhaust valves. This suggests that it may be possible to improve the thermodynamic efficiency of such 2-stroke mode by increasing the expansion process through retarded exhaust opening. Such change may not be desirable for the SI combustion due to the deteriorating scavenging process but it could be implemented for CAI combustion which relishes the presence of hot residual gases. In the 2-stroke CAI mode, the combustion occurs too early, which is reflected by the CA50 shown in Figure 11 and leads to the low thermodynamic efficiency.

NET INDICATED EFFICIENCY

Combining the efficiencies above, the net indicated efficiency can be worked out and their values are shown in Figure 12. Figure 13 shows the Indicated Specific Fuel Consumption (ISFC) of the seven operating modes, which is calculated from the ratio of fuelling rate to the indicated power.

In 4-stroke modes, the net indicated efficiency of the throttle controlled SI is the lowest due to the high pumping loss and low thermal efficiency, hence the higher fuel consumption. Intake valve throttled SI mode increases the net indicated efficiency by less than 1% at this operating condition since the reduced pumping work is offset by the reduction in the combustion efficiency. With reduced pumping loss, 4-stroke positive valve overlap SI mode exhibits the same indicated efficiency as the 4-stroke negative valve overlap CAI mode. 4-stroke CAI operation with exhaust rebreathing shows the highest net indicated efficiency and thus the lowest fuel consumption, due to the absence of pump loss and faster combustion.

The 2-stroke SI has the lowest indicated efficiency of the seven operation modes due to its low combustion efficiency and thermodynamic efficiency. At the same power output, the Indicated efficiency in the 2-stroke mode is lower than that of the 4-stroke due to the lower expansion ratio. But at the same IMEP, the highest indicated efficiency and hence the lowest ISFC are obtained with the 2-stroke CAI combustion, as shown in Fig.12 (b) and Fig.13 (b).

EMISSIONS

As shown in Figure 9, CAI combustion generates similar CO or HC emissions to those of SI operations. High CO and HC emissions are mainly caused by the poor mixing or substantial diffusion combustion from any liquid fuel film formed on the piston crown. It is noted that as the injection takes place earlier CO emissions tend to fall due to the longer mixing period. There is no obvious evidence in fuel short-circuiting in the 2-stroke modes as was the case of conventional port injected 2-stroke engine operations.

NO_x emission data in Figure 14 shows that 4-stroke intake valve throttled SI combustion produces slightly lower NO_x emission owing to the lower in-cylinder temperature of the shorten compression process by the retarded intake valve closing time. Because of the presence of a large quantity of recycled burnt gas, the NO_x emission is significantly reduced in both 4-stroke CAI modes as well as the 2-stroke SI and CAI modes.

MECHANICAL EFFICIENCY AND BRAKE SPECIFIC FUEL CONSUMPTION

Friction Power (Pf) calculated from the difference between engine brake output and indicated output is shown in Figure 15. For 2-stroke operation modes, the work consumed by the supercharger for scavenging is calculated from the pressure difference between the inlet and outlet port of the supercharger and included in Pf. An engine driven mechanical supercharger was assumed with an overall efficiency of 60%. As it can be seen from Fig.15, the intake valve throttled SI operation has the lowest friction in 4-stroke operations due to the lower in-cylinder pressure. The Pf values of 2-stroke operation modes are higher than that of 4-stroke operation modes because of the mechanical

supercharger power consumption. This causes 7% decrease in Mechanical efficiency of 2-stroke CAI and SI at the same power output, as shown in Figure 16. However, it would be possible to minimize such losses by employing a turbocharger in place of the supercharger.

Figure 17 shows the Brake Specific Fuel Consumption (BSFC) in the seven operation modes, which is calculated from the ratio of the fuelling rate to the brake power obtained from the engine crankshaft. This reflects the total fuel consumption after taking the friction loss and the supercharger power into account. The 4-stroke exhaust rebreath CAI operation mode has the best fuel economy and reduces the fuel consumption by 11.9% compared with 4-stroke throttle controlled SI operation mode. In the 2-stroke operation, as the engine operated at half IMEP load point of 4-stroke operations where mechanical efficiency and thermodynamic efficiency were lower than that of 4-stroke, the BSFC increased by 4.4% for CAI and 20.7% for SI. However, if 50% engine downsizing is adopted by a 2-stroke engine in place of a larger 4-stroke engine, the 2-stroke CAI operation will result in 29% reduction in BSFC at the same IMEP value.

CONCLUSIONS

By altering the intake and exhaust valve events through a fully flexible hydraulic VVA system, seven operation modes were realised in a single cylinder direct injection gasoline engine. Their efficiencies and emission results are presented and analysed in this paper. The main findings can be summarised as follows:

1. The 4-stroke throttle controlled SI operation mode has the highest pumping loss due to the partially closed throttle. The 4-stroke exhaust rebreathing CAI operation mode has the lowest pumping loss when the exhaust gases are re-circulated during the intake stroke.
2. The 2-stroke SI has the lowest combustion efficiency due to slow and in-complete combustion.
3. The 4-stroke exhaust rebreathing CAI has the highest indicated efficiency due to the lowest pumping loss and higher thermodynamic efficiency caused by the shorter combustion duration. The 2-stroke SI has the lowest indicated efficiency due to the low combustion efficiency and thermodynamic efficiency.
4. The 2-stroke operation modes produce more CO emissions due to the shortened mixing process. Without the dilution of exhaust gases, 4-stroke throttle controlled SI and intake valve throttled SI combustion produce more NOx emission.
5. The 2-stroke CAI combustion will be most suited for part-load operations in a highly downsized DI gasoline engine and its overall efficiency can be further improved through turbocharging.

ACKNOWLEDGMENTS

The authors would like to acknowledge the financial support granted by Engineering and Physical Sciences Research Council (EPSRC), UK, and the technical support to the engine control by Ricardo UK.

REFERENCES

1. Flierl R., et al. The Third Generation of Valvetrains-New Fully Variable Valvetrains for Throttle-Free Load Control. SAE Paper 2000-01-1227, 2000.
2. Takemura, S., Aoyama, S., Sugiyama, T., Nohara, T., Moteki, K., Nakamura, M., and Hara, S., A Study of a Continuous Variable Valve Event and Lift (VEL) System, SAE Paper 2001-01-0243, 2001.
3. Kawasumi, I., and Yasui, Y., Adaptive Air-Fuel Ratio Controls for Continuously Variable Valve Lift Gasoline Engines, SAE Paper 2007-01-1198, 2007.
4. Ha K., Han D., and Kim W., Development of Continuously Variable Valve Lift Engine, SAE paper, 2010-01-1187, 2010.
5. Kinoshita K., et al, Development of a Custom Integrated Circuit for Continuously Variable Valve Lift Mechanism System Control, SAE paper 2008-01-0913, 2008.
6. Allen J., et al. Production Electro-Hydraulic Variable Valve-Train for a New Generation of I.C. Engines. SAE Paper 2002-01-1109, 2002.
7. Miller, et al. Electromechanical valve assembly for an internal combustion engine. U.S. patent 6,795,291 (Sep. 21, 2004).
8. Diehl, et al. Internal combustion engine. U. S. patent 6,701,879 (Mar. 9, 2004).
9. Zhao F., Asmus, T.W., Assanis, D.N., Dec, J.E., Eng, J.A., Najt, P.M., Homogeneous Charge Compression Ignition (HCCI) Engines, Key Research and Development Issues, SAE Publication PT-94, Soc. of Automotive Engineers, 2003.
10. Zhao H. (ed.), HCCI and CAI engines for the Automotive Industry, Woodhead Publishing, Cambridge, 2007.

11. Milovanovic N. et al, Cam Profile Switching (CPS) and Phasing Strategy vs Fully Variable Valve Train (FVVT) Strategy for Transitions between Spark Ignition and Controlled Auto Ignition Modes, SAE paper 2005-01-0766, 2005.
12. A. Fuerhapter, W.F. Piock, G.K. Fraidl, CSI-Controlled Auto Ignition – the Best Solution for the Fuel Consumption - Versus Emission Trade off? SAE paper 2003-01-0754, 2003.
13. Wolters P., Salber W., Geiger J. et al, Controlled Auto Ignition Combustion Process with an Electromechanical Valve Train, SAE paper 2003-01-0032, 2003.
14. Osborne R. J., Stokes J., Lake T. H., et al, Development of a Two-Stroke/Four-Stroke Switching Gasoline Engine - The 2/4SIGHT Concept, SAE paper 2005-01-1137, 2005.
15. Zhang, Y., Ojapah, M., Cairns, A., and Zhao, H., 2-Stroke CAI Combustion Operation in a GDI Engine with Poppet Valves, SAE Technical Paper 2012-01-1118, 2012, doi:10.4271/2012-01-1118.
16. Zhang Y. and Zhao H., Measurement of short-circuiting and its effect on CAI or HCCI combustion in a two-stroke poppet valve engine, Proceedings of the Institution of Mechanical Engineers, Part D: Journal of Automobile Engineering, February, 2012, doi:10.1177/0954407011434252.
17. Zhang, Y. and Zhao, H., Lean Boost CAI Combustion in a 2-stroke Poppet Valve GDI Engine, To be presented in IMechE conference, 'Internal Combustion Engines: Performance, Fuel Economy and Emissions.' Nov., 2013.

CONTACT

Dr. Y. Zhang

Centre for advanced powertrain and fuel research (CAPF),

Brunel University London, UK

UB8 3PH

Yan.zhang@brunel.ac.uk

DEFINITIONS, ACRONYMS, ABBREVIATIONS

4str	4-stroke
2str	2-stroke
BDC	Bottom dead centre
TDC	Top dead centre
PVO	Positive valve overlap
NVO	Negative valve overlap
IVL	Intake valve lift
IVO	Intake valve open
IVC	Intake valve close
EVO	Exhaust valve open
EVC	Exhaust valve close
CAI	Controlled auto ignition
SI	Spark ignition
EGR	Exhaust gas recirculation
ISFC	Indicated specific fuel consumption
BSFC	Brake specific fuel consumption
IMEP	Net indicated mean effective pressure

IMEP _{gross}	Gross indicated mean effective pressure
PMEP	Pumping mean effective pressure
BMEP	Brake mean effective pressure
FMEP	Friction mean effective pressure
CA10	10% mass fuel burnt crank angle
CA50	50% mass fuel burnt crank angle
CA90	90% mass fuel burnt crank angle
ISHC	Indicated specific hydrocarbon
ISCO	Indicated specific carbon monoxide
ISNOx	Indicated specific nitric oxide

APPENDIX

UNCERTAINTIES OF ALL MEASUREMENT VARIABLES

Device		Maximum measured error
In-cylinder pressure transducer		± 0.5% of Full scale
Intake pressure transducer		± 0.1% of Full scale
Exhaust pressure transducer		± 0.1% of Full scale
Dyno torque sensor		± 0.05% of Full scale
Fuel flow meter		± 0.10% + [(0.0025kg/h ÷ measured value in kg/h) · 100]%
Air flow meter		± 1% of Full scale
Fuel pressure transducer		± 0.3% of Full scale
K type thermocouples		± 0.75% of reading
Gas analyser	CO2	± 1% of full scale or ± 2% of reading (whichever is smaller)
	CO	
	THC	
	NO	
	N2O	
	O2	

FORMULAS OF THE EFFICIENCIES

$$1. \text{ IMEP} = \begin{cases} \int_{-180}^{540} \frac{p}{V_s} \dot{V}(\varphi) d\varphi & (4 - \text{stroke}) \\ \int_{-180}^{180} \frac{p}{V_s} \dot{V}(\varphi) d\varphi & (2 - \text{stroke}) \end{cases}$$

Where, Vs, displacement of the engine.

$$2. \text{ IMEP}_{\text{gross}} = \int_{-180}^{180} \frac{p}{V_s} \dot{V}(\varphi) d\varphi$$

$$3. \text{ PMEP} = \text{IMEP} - \text{IMEP}_{\text{gross}}$$

$$4. \text{ Gas exchange efficiency} = \text{IMEP}_{\text{gross}} / \text{IMEP}$$

$$5. \text{ Combustion efficiency} = 1 - (G_{\text{CO}} \cdot 10.1 + G_{\text{HC}} \cdot 43) / (\text{Fuel flow rate} \cdot \text{LHV})$$

Where,

G_CO, CO emission mass flow rate

G_HC, HC emission mass flow rate

LHV, Low heat value of the fuel

6. Thermodynamic efficiency= $IMEP_{gross} / (\text{Fuel flow rate} * LHV / V_s * \text{Combustion efficiency})$

7. Work consumed by the supercharger:

$$W_c = \text{Air flow rate} * C_p * T_1 * \left[\left(\frac{P_2}{P_1} \right)^{\frac{\gamma-1}{\gamma}} - 1 \right] / \eta_c / \eta_{mechanical}$$

Where,

For the air, $C_p = 1.012 \text{ J/(g.K)}$

$\gamma = 1.4$

Compressor efficiency: $\eta_c = 60\%$

Compressor Mechanical efficiency: $\eta_{mechanical} = 90\%$

T1, Supercharger inlet temperature

P1, Supercharger inlet pressure

P2, Supercharger outlet pressure

8. Mechanical efficiency= $(BMEP - W_c / V_s) / IMEP$

Figure Captions

Figure 1 Single Cylinder Camless DI gasoline engine and combustion chamber

Figure 2 Valve timings and Injection timings for the 7 operation modes

Figure 3 In-cylinder pressure traces of 2 and 4 strokes engine operations

Figure 4 Heat release rate curves

Figure 5 P-V diagrams for 7 operation modes at the same power output

Figure 6 PMEP of 7 operation modes

Figure 7 Gas exchange efficiency of 7 operating modes

Figure 8 Combustion efficiency in 7 operating modes

Figure 9 ISCO and ISHC of 7 operating modes

Figure 10 Gross indicated thermodynamic efficiency of 7 operating modes

Figure 11 CA50 of 7 operating modes

Figure 12 Net Indicated Efficiency of 7 operating modes

Figure 13 ISFC of 7 operating modes

Figure 14 NOx emissions of 7 operation modes

Figure 15 Friction Power of 7 operation modes

Figure 16 Mechanical Efficiency of 7 operation modes

Figure 17 BSFC of 7 operating modes based on supercharged 2-stroke operations

Figure

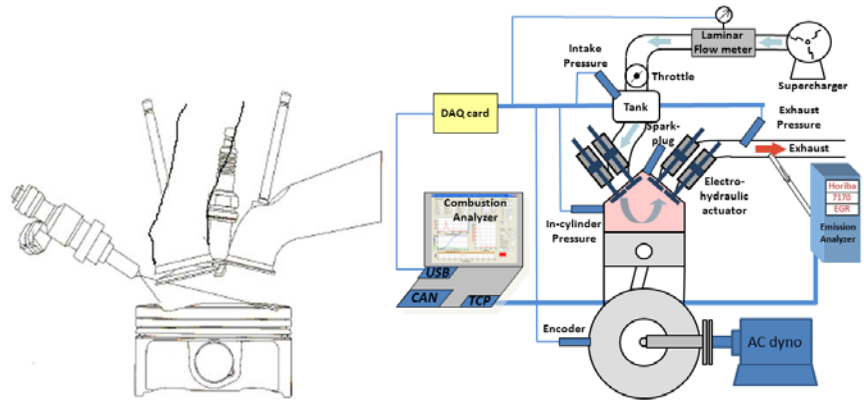
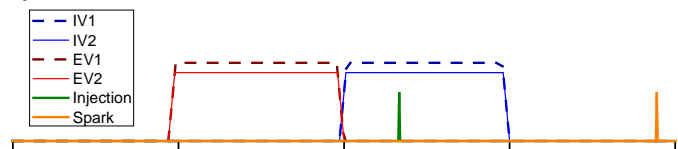
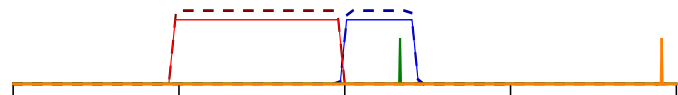


Figure 1 Single Cylinder Camless DI gasoline engine, combustion chamber and experimental Setup

1) 4-stroke Throttle-controlled SI



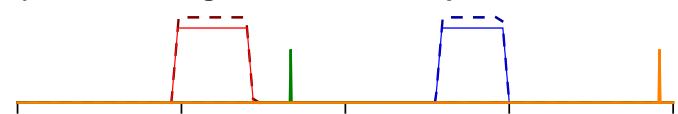
2) 4-stroke Intake valve throttled SI



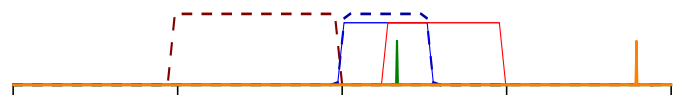
3) 4-stroke Positive Valve Overlap SI



4) 4-stroke Negative Valve Overlap CAI



5) 4-stroke Exhaust Rebreath CAI



6) 2-stroke CAI



7) 2-stroke SI

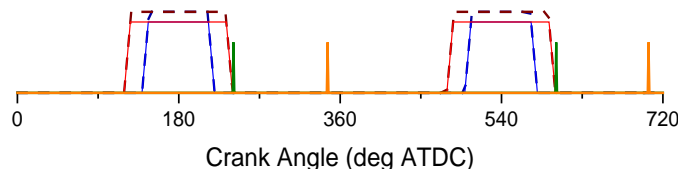
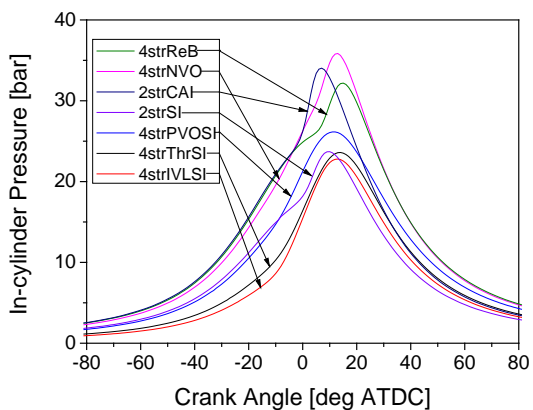
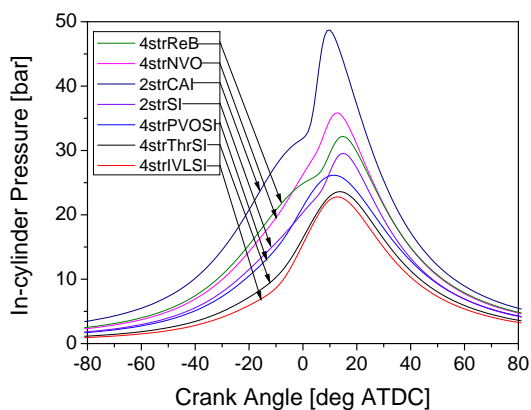


Figure 2 Valve timings and Injection timings for the 7 operation modes

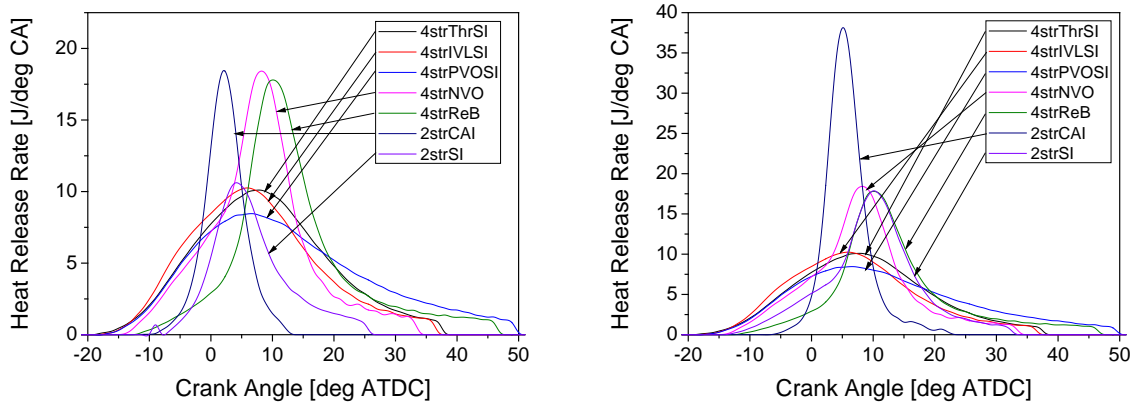


(a) Pressure curves at the same power



(b) Pressure curves at the same IMEP

Figure 3 In-cylinder pressure traces of 2 and 4 strokes engine operations



(a) Heat release rates at the same power

(b) Heat release rates at the same IMEP

Figure 4 Heat release rate curves

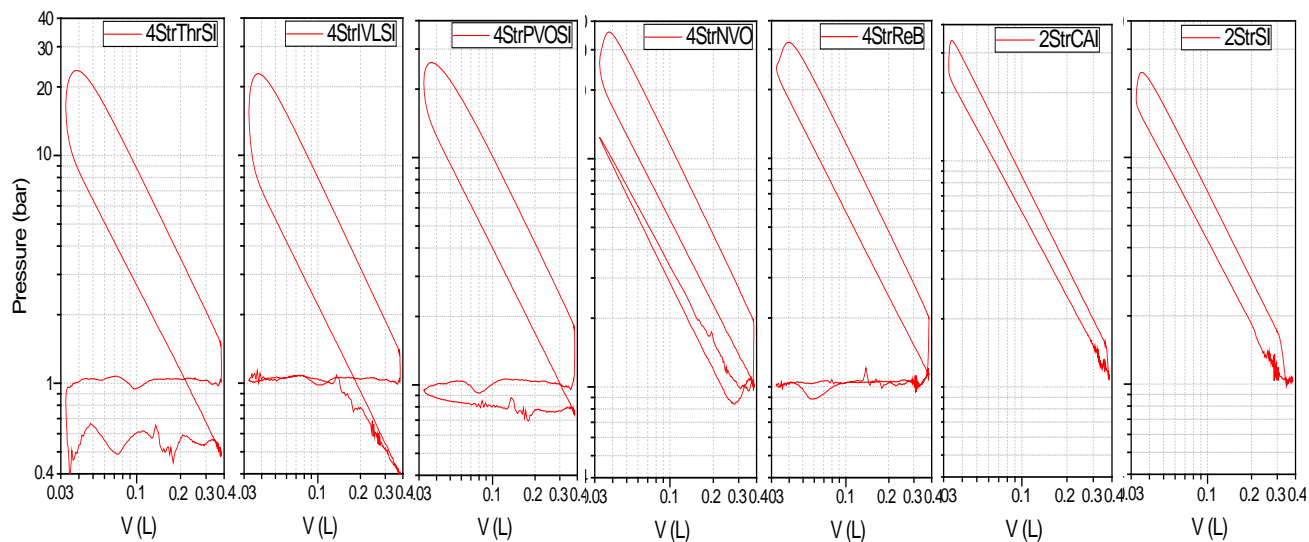


Figure 5 P-V diagrams for 7 operation modes at the same power output

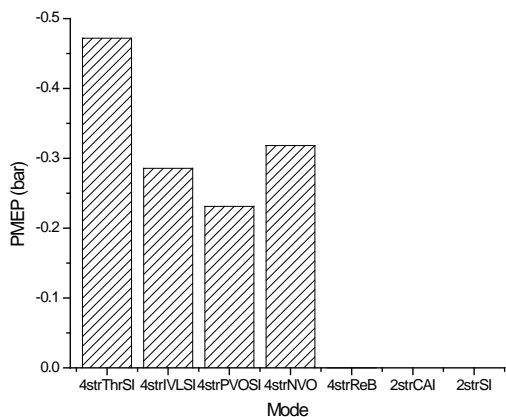


Figure 6 PMEP of 7 operation modes

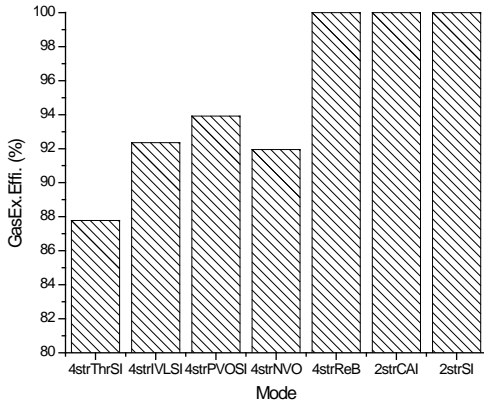
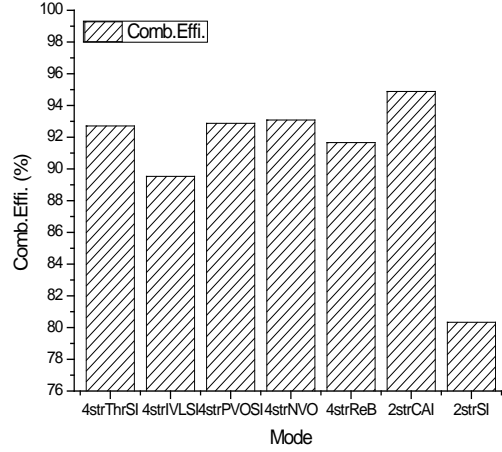
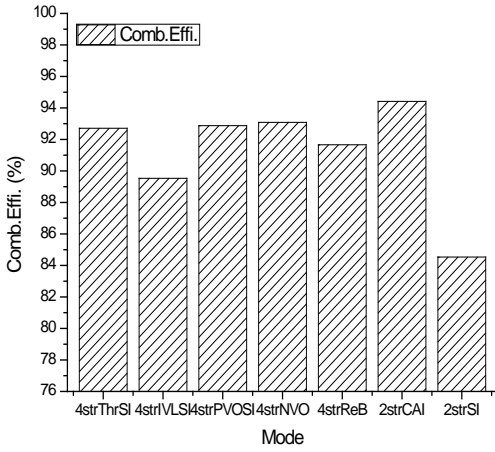


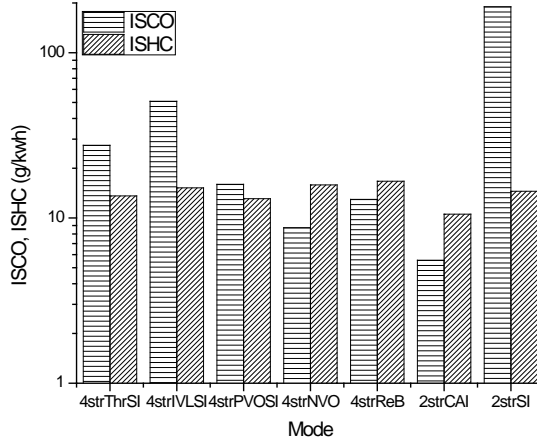
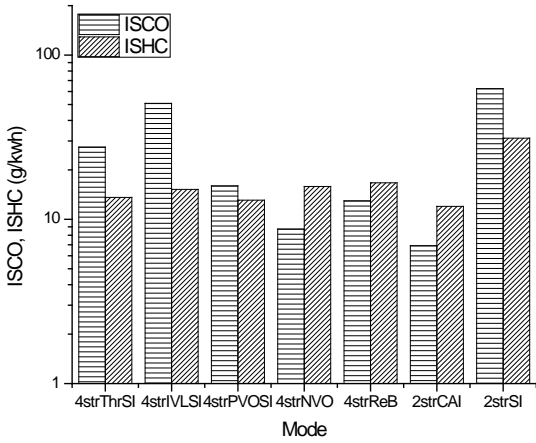
Figure 7 Gas exchange efficiency of 7 operating modes



(a) Combustion efficiency at the same power

(b) Combustion efficiency at the same IMEP

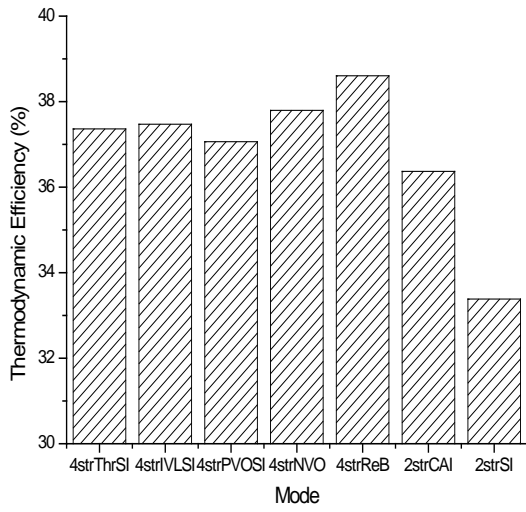
Figure 8 Combustion efficiency in 7 operating modes



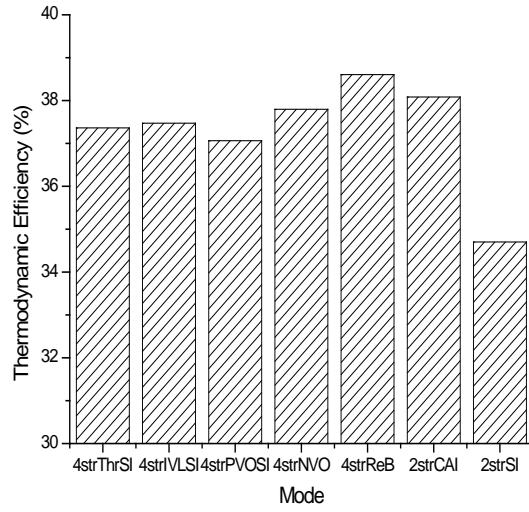
(a) CO and HC emissions at the same power

(b) CO and HC emissions at the same IMEP

Figure 9 ISCO and ISHC of 7 operating modes

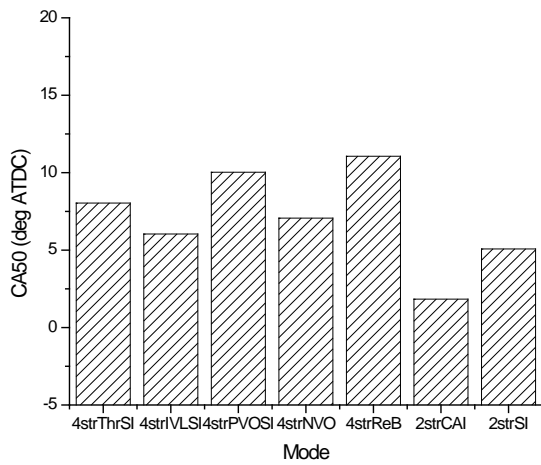


(a) Gross efficiency at the same power

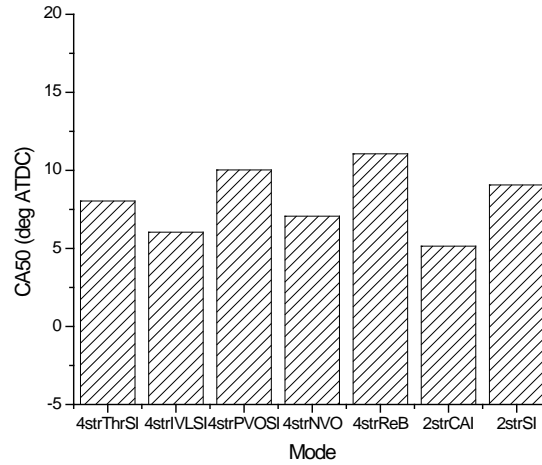


(b) Gross efficiency at the same IMEP

Figure 10 Gross indicated thermodynamic efficiency of 7 operating modes

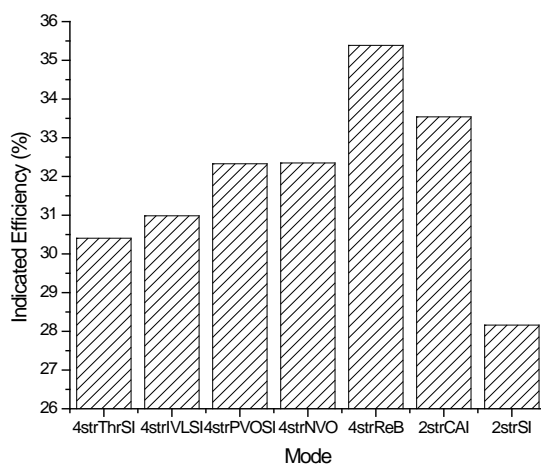


(a) CA50 at the same power

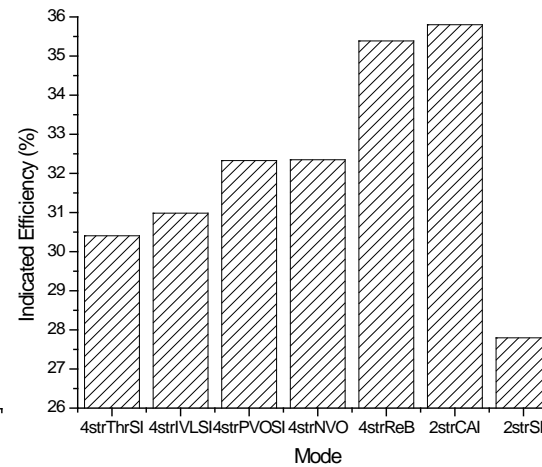


(b) CA50 at the same IMEP

Figure 11 CA50 of 7 operating modes

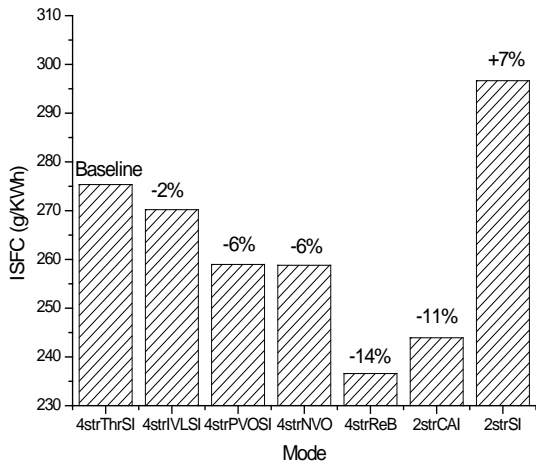


(a) Indicated efficiency at the same power

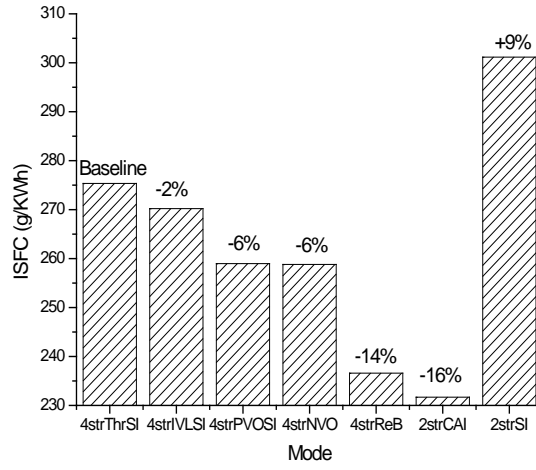


(b) Indicated efficiency at the same IMEP

Figure 12 Net Indicated Efficiency of 7 operating modes

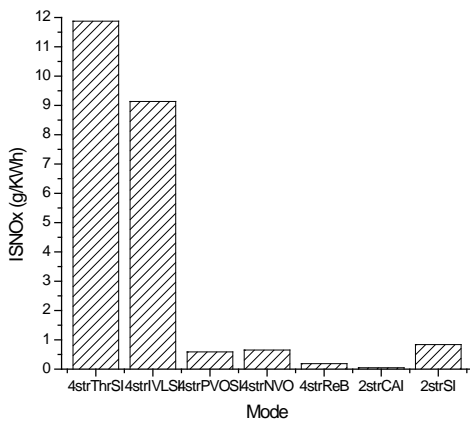


(a) ISFC at the same power

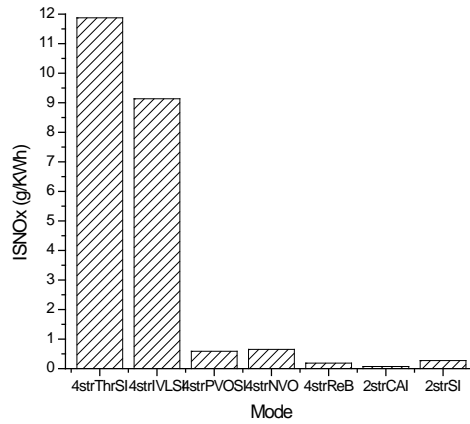


(b) ISFC at the same IMEP

Figure 13 ISFC of 7 operating modes

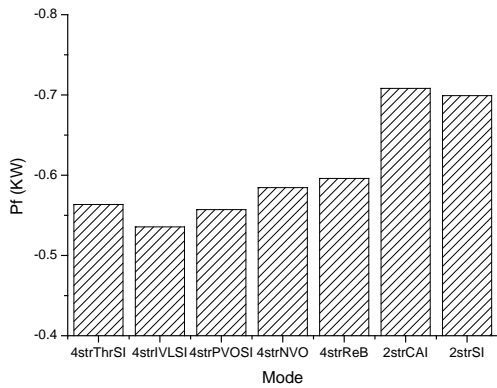


(a) NOx emissions at the same power

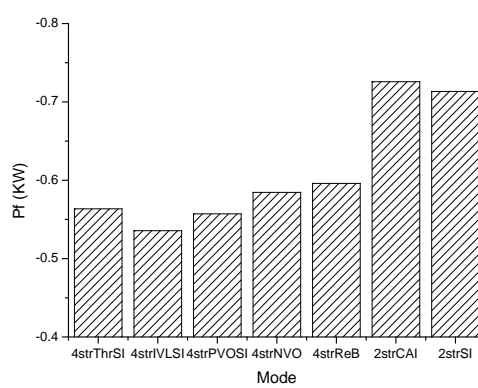


(b) NOx emissions at the same IMEP

Figure 14 NOx emissions of 7 operation modes

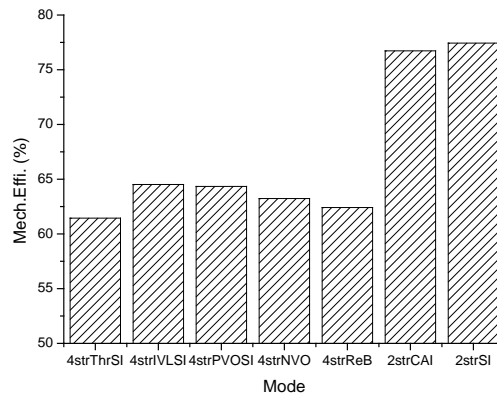
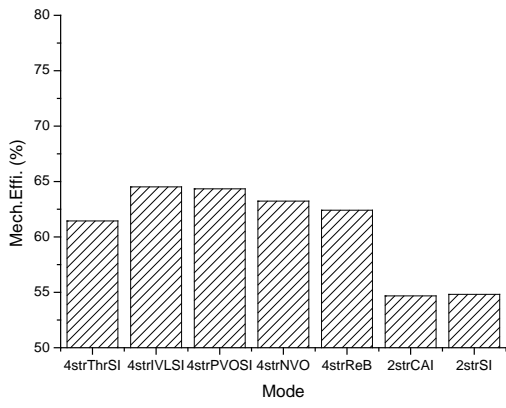


(a) Friction and supercharger power at the same power



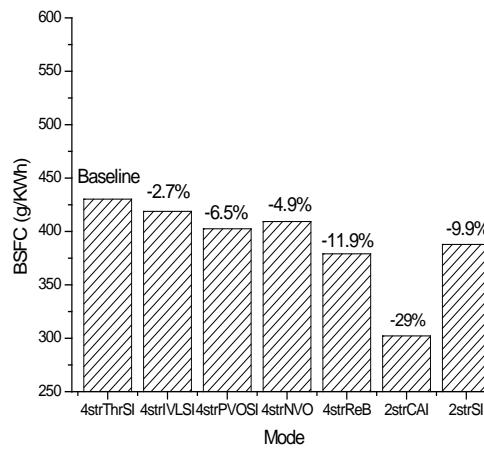
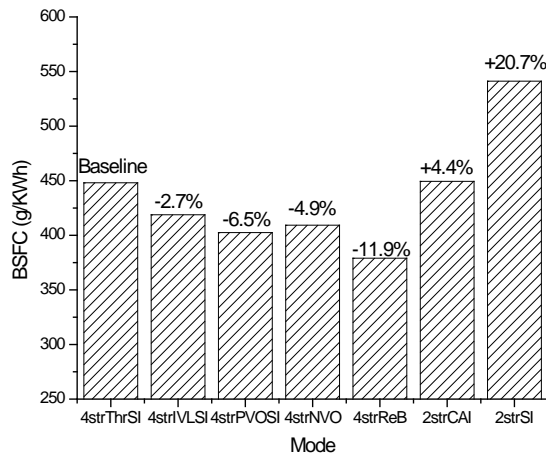
(b) Friction and supercharger power at the same IMEP

Figure 15 Friction Power of 7 operation modes



(a) Mechanical efficiency at the same power (b) Mechanical efficiency at the same IMEP

Figure 16 Mechanical Efficiency of 7 operation modes



(a) BSFC at the same power (b) BSFC at the same IMEP

Figure 17 BSFC of 7 operating modes based on supercharged 2-stroke operations

Tables

Table 1 Engine specifications

Bore x Stroke	81.6mmx66.94mm
Swept volume	0.35L
Compression ratio	11.78:1
Combustion chamber	Pent roof / 4 valves
Valve train	Electro-hydraulic actuation
Fuel injection	Direct injection
Fuel	Standard gasoline (RON 95)
Injection Pressure	100bar
Intake temperature	25°C

Table 2 Engine operating conditions

Mode	IMEP	Speed	Pi	Spark Timing	Air/Fuel mixture	COV _{MEP}	IVO	IVC	EVO		EVC		Boost Pressure
	bar	r/min	KW	Deg. ATDC	Lambda, □	%							
4sThr-SI	3.6	1500	1.57	-20	Stoichiometric	1.7	5deg BTDC	0deg ABDC	10deg BBDC	0deg ATDC			NA
4sIVL-SI	3.6	1500	1.57	-16	Stoichiometric	2.3	5deg BTDC	100deg BBDC	10deg BBDC	0deg ATDC			NA
4sPVO-SI	3.6	1500	1.57	-25	Stoichiometric	5.7	30deg BTDC	0deg ABDC	10deg BBDC	25deg ATDC			NA
4sNVO-CAI	3.6	1500	1.57	-17 (less effective)	Stoichiometric	1.7	100deg ATDC	0deg ABDC	10deg BBDC	100deg BTDC			NA
4sReB-CAI	3.6	1500	1.57	-38 (less effective)	Stoichiometric	3.7	5deg BTDC	80deg BBDC	No.1	No.2	No.1	No.2	NA
									10deg BBDC	45deg ATDC	0deg ATDC	0deg ABDC	
2s-CAI	3.6	1500	3.14	-9 (less effective)	~Stoichiometric	1.3	20deg BBDC	40deg ABDC	40deg BBDC		20deg ABDC		1.779
	1.8	1500	1.57	-17 (less effective)	~Stoichiometric	2.1							1.250
2s-SI	3.6	1500	3.14	-14	~Stoichiometric	2	40deg BBDC	40deg ABDC	60deg BBDC		60deg ABDC		1.058
	1.8	1500	1.57	-8	~Stoichiometric	7.6							1.046